GWAS and WGCNA uncover hub genes controlling salt tolerance in maize (*Zea mays L.*) seedlings

Langlang Ma
Sichuan Agricultural University

Minyan Zhang
Sichuan Agricultural University - Chengdu Campus

Jie Chen
Sichuan Academy of Agricultural Science

Chunyan Qing
Sichuan Agricultural University - Chengdu Campus

Shijiang He
Sichuan Agricultural University

Changying Zou
Sichuan Agricultural University

Guangsheng Yuan
Sichuan Agricultural University

Cong Yang
Sichuan Agricultural University

Hua Peng
Sichuan Tourism College

Guangtang Pan
Sichuan Agricultural University

Thomas Lübberstedt
Iowa State University

Yaou Shen (✉ shenyaou@sicau.edu.cn)
Sichuan Agricultural University   https://orcid.org/0000-0001-7603-0108

Research Article

Abstract

Salt stress influences maize growth and development. To decode the genetic basis and hub genes controlling salt tolerance is a meaningful exploration for cultivating salt-tolerant maize varieties. Herein, we used an association panel consisting of 305 lines to identify the genetic loci responsible for Na^+- and K^+-related traits in maize seedlings. Under the salt stress, seven significant single nucleotide polymorphisms were identified using a genome-wide association study, and 120 genes were obtained by scanning the linkage disequilibrium regions of these loci. According to the transcriptome data of the above 120 genes under salinity treatment, we conducted a weighted gene co-expression network analysis. Combined the gene annotations, two SNaC/SKC (shoot Na^+ content/shoot K^+ content)-associated genes *GRMZM2G075104* and *GRMZM2G333183* were finally identified as the hub genes involved in salt tolerance. Subsequently, these two genes were verified to affect salt tolerance of maize seedlings by candidate gene association analysis. Haplotypes TTGTCCG-CT and CTT were determined as favorable/salt-tolerance haplotypes for *GRMZM2G075104* and *GRMZM2G333183*, respectively. These findings provide novel insights into genetic architectures underlying maize salt tolerance and contribute to the cultivation of salt-tolerant varieties in maize.

Key Message

Two hub genes *GRMZM2G075104* and *GRMZM2G333183* involved in salt tolerance were identified by GWAS and WGCNA. Furthermore, they were verified to affect salt tolerance by candidate gene association analysis.

Introduction

Salinity is a major abiotic stress affecting crop growth, development, and yield (Cui et al. 2015; Zhu 2001). Globally, approximately 50% of irrigated lands and 20% cultivated lands are affected by salt stress (Hu and Schmidhalter 2005; Luo et al. 2019a). As an important crop, maize is sensitive to salt stress, particularly at the seedling stage (Cui et al. 2015). Understanding the genetic architecture and causal genes of salt tolerance in maize seedlings is an urgent need to reduce salinity damage and cultivate salt-tolerant maize cultivars for breeders.

Two important mechanisms underlying the response of salinity stress have been widely verified in plants, namely SOS (salt overly sensitive) and HKT (high-affinity K^+ transporter) pathways (Hamamoto et al. 2015; Zhu 2002). In SOS pathway, three genes *SOS1*, *SOS2*, and *SOS3* jointly participate in the plant metabolism under salt stress (Zhu 2002). As a Na^+/K^+ transporter, *SOS1* is specifically expressed in root tips, and epidermal cells of stems and leaves (Shi et al. 2000; Shi et al. 2002). Under salinity stress, *SOS1* transports Na^+ out of cells via H^+ electrochemical potential (Shi et al. 2002). *SOS2* and *SOS3* encode Serine/Threonine protein kinase and calcium-binding protein with EF hand motifs, respectively (Halfter et al. 2000; Liu et al. 2000). During salt stress, Ca^{2+} activates *SOS2* and causes the formation of *SOS2-SOS3* complex, which then activates the C-terminal region of *SOS1* by phosphorylation (Quintero et al. 2011).

Proteins MPK6 and SCaBP also participate in the SOS pathway (Ji et al. 2013). HKT is an Na^+-preferential transporter, which mainly controls root-shoot Na^+ delivery after the Na^+ transits xylem and gets into the cell (Munns 2002; Ren et al. 2005; Zhang et al. 2018). Additionally, IAA (auxin), ABA (abscisic acid), ETH (ethylene) and other plant hormones were reported to be the key regulators in the responses of salt stress (Ryu and Cho 2015).

Linkage mapping is a useful method to dissect the genetic basis of quantitative traits (Cui et al. 2015). Currently, numerous quantitative trait loci (QTL) controlling salt tolerance have been identified in crops by linkage mapping. In rice, *SKC*1 was the first cloned QTL for salt tolerance in rice (Ren et al. 2005). Using a RIL ($F_{2:9}$) population detected 16 QTL associated with rice salt-tolerance (Wang et al. 2011). Hamwieh and Xu (2008) uncovered a major salt-tolerant QTL, which explained 68.7% of phenotypic variation in Soybean. In maize, Hoque (2013) identified 10 salt tolerance QTL in an F_2 population consisting of 163 lines. QTL analyses using an $F_{2:5}$ population revealed eight QTL related to salt tolerance-related traits (Cui et al. 2015). Recently, Zhang et al. (2018) cloned a salt tolerance-associated gene *HKT1* based on QTL fine-mapping in maize. However, only a few QTL (*SKC*1 in rice and *HKT1* in maize) were fine-mapped and cloned in crops, owing to the large confidence intervals of these QTL (Ren et al. 2005; Zhang et al. 2018). Genome-wide association studies (GWAS) provide the detection of QTL with a high-resolution approach (Sukumaran et al., 2015) and have been extensively used for excavating the candidate genes controlling targeted traits (Korte and Farlow 2013). Using GWAS, 66 significant single nucleotide polymorphisms (SNPs) were found to be associated with 12 salt tolerance traits in rice (Kumar et al. 2015). In barley, GWAS using 2,671 lines detected a salt tolerance-associated gene *HKT1;5* (Hazzouri et al. 2018). In maize, a Na^+ transport-associated gene *HAK4* was identified via GWAS and subsequently functionally-validated by overexpression and mutant strategies (Zhang et al. 2019). Weighted gene co-expression network analysis (WGCNA) facilitates the revelation of the core gene networks based on the gene expression patterns from RNA-seq data, which has become a favored and popular technique in discovering hub factors controlling traits (Wan et al. 2018; Guo et al. 2020). Liu et al. (2016a) identified six priority transcription factors associated with lysine biosynthesis in the LBPGs module of WGCNA results. Two hub genes involved in element accumulations were detected using WGCNA and further verified by a mutant-based approach (Schaefer et al. 2018).

In plants, salt tolerance was previously evaluated by several traits, such as shoot fresh weight, shoot dry weight, plant height, etc (Cui et al. 2015; Kumar et al. 2015). By contrast, Na^+ and K^+ accumulations are more direct and important traits for salt tolerance due to their important roles in regulating osmotic tolerance and Na^+/K^+ delivery under salt stress (Zhang et al. 2018). In the present study, GWAS was performed in a panel consisting of 305 individuals to detect significant SNPs correlating with Na^+ and K^+ accumulations under salinity conditions. Subsequently, expression values of these candidate genes were utilized to carry out WGCNA for identifying the priority genes. Finally, the target genes were individually PCR-amplified among 77 randomly selected lines from the association panel and the variation loci for each gene were then subjected to candidate gene association analysis. The goal of this study was to

determine the hub candidate genes affecting Na^+- and K^+-related traits and identify the favorable haplotypes of the hub genes for improving the salt tolerance in maize breeding.

Materials And Methods

Plant materials and trait measurements

An association panel including 305 inbred lines was used to carry out GWAS in this study. This panel was composed of tropical, stiff stalk (SS), non-stiff stalk (NSS), and other germplasms (Zhang et al. 2016).

A randomized complete block design was used for the trials with three replications for each line. Thirty kernels of each line were treated with 10% H_2O_2 for 10 min and then soaked with saturated $CaSO_4$ for 12 h. After being rinsed three times by deionized water, the seeds were placed on vermiculites for germination in the growth chamber with a 16/8 h light/darkness cycle, a 25/22°C day/night temperature cycle, a 200 µmol photonsm^{-2} s^{-1} brightness, and a relative humidity of 65 % (Ma et al. 2020). At the three-leaf stage, the seedlings were divided into two groups and separately cultivated in Hoagland's solutions (normal treatment, NT) and Hoagland's solutions containing 150 mM NaCl (salt stress, SS) for 7d. The formulas of Hoagland's solution were described by Cui et al. (2015). In each line, eight seedlings with healthy and consistent growth for each treatment were selected and then kept in an oven at 80 °C for 72 h.

The dried shoots and roots were respectively crushed and approximately 2 g power of per sample were diluted with 80% H_2SO_4 for extracting Na^+ and K^+ by MARS6 instrument. Inductively Coupled Plasma Mass Spectrometer (ICP-MS) was used to measure Na^+ and K^+ contents.

Phenotypic data analysis

In each condition, eight traits were collected in this study. These were shoot Na^+ content (SNaC), root Na^+ content (RNaC), shoot K^+ content (SKC), root K^+ content (RKC), shoot Na^+ content/shoot K^+ content (SNaC/SKC), root Na^+ content/root K^+ content (RNaC/RKC), K^+ transport coefficient (KTC, shoot K^+ content/root K^+ content), Na^+ transport coefficient (NaTC, shoot Na^+ content/root Na^+ content).

The mean value, standard deviation (SD), maximum value, and minimum value of each trait were calculated by Microsoft Excel. SPSS software (Statistical Product and Service Solutions, version 21.0, IBM, Armonk, NY) was used to analyze the correlations of the collected traits and compare the phenotypes between two treatments (normal and salt treatments) for each trait by t-test. Analysis of variance (ANOVA) was based on the model $y_{ij} = \mu + R_i + G_j + E_{ij}$. Here y_{ij}, μ, R_i, G_j, and E_{ij} denote the observation from the ijth plot, the overall mean, the effect of the ith replication, the effect of the jth genotype, and the experimental error, respectively (Ma et al. 2020). SAS 9.3 (Statistical Analysis System, version 9.3, SAS Institute, Cary, NC, USA) was utilized to estimate the broad-sense heritability (H^2), which was described as follows (Pace et al. 2015):

$$H^2 = \frac{\sigma_G^2}{\sigma_P^2}, \quad \sigma_G^2 = \left(\frac{MSG - MSE}{rep}\right), \quad \sigma_P^2 = \left(\frac{MSG - MSE}{rep}\right) + MSE, \quad H^2 = \frac{\left(\frac{MSG - MSE}{rep}\right)}{\left(\frac{MSG - MSE}{rep}\right) + MSE}$$

Where, σ_G^2, σ_P^2, MSG, MSE, and rep represent genotype variance, phenotype variance, mean square of genotype, mean square of error, and the replication numbers (= 3), respectively.

Genotypic data analysis

Genotypic data of the 305 accessions were obtained using the Illumina MaizeSNP50 BeadChip, as described in our previous study (Zhang et al. 2016). A total of 46, 408 SNPs evenly distributed over 10 chromosomes were remained after removing the SNPs with missing rate > 20%, heterozygosity > 20%, or minor allele frequency (MAF) < 0.05. In previous studies, evaluation of population structure and linkage disequilibrium (LD) in this panel revealed that the 305 lines can be divided into three subgroups and the LD decay approximately reached to 300 Kb (r^2 = 0.1) (Zhao et al. 2018; Zhang et al. 2020a). Thus, PCA (principal component analysis) = 3 was used as a covariate in GWAS, and LD = 300 Kb was used for excavating candidate genes in this study.

GWAS

Currently, three models were adopted in GWAS, namely GLM (General Linear Model), FarmCPU (Fixed and random model Circulating Probability Unification) model, and MLM (Mixed Linear Model). GLM trends to generate false positives due to no covariates included in this model, whereas MLM results in many false negatives due to the stringent redresses of population structure (Q matrix) and kinship (K matrix) (Hu et al. 2017; Ma et al. 2020). FarmCPU model addresses the confounding problem of testing markers using iterative algorithms, which is moderately stringent in comparison to GLM and MLM (Liu et al. 2016b; Ma et al. 2020). Consequently, FarmCPU model was used in this study for GWAS. As a covariate, PCA was calculated by GAPIT software (Lipka et al. 2012) and then added to FarmCPU model. GAPIT software and FarmCPU model were both run in R studio (version 3.4.1). Herein, the significance threshold was set as: P-value = 0.05/n (n is the total SNP number) = 0.05/46,408 = 1.08×10^{-6}. SNPs with P-value < 1.08×10^{-6} were considered as the significant SNP-trait associations. Moreover, the genes located in the LD regions of the significant SNPs were identified as candidate genes affecting traits.

WGCNA and hub gene identification

The gene expression values were obtained from RNA-seq in our previous study (Accession number: CRA003872; Zhang et al. 2021). Briefly, the seeds of L2010-3 (a salt-tolerant line) and BML1234 (a salt-sensitive line) were germinated in a growth chamber. At two-leaf stage, the seedlings were divided into two groups and respectively transplanted into Hoagland's solutions (control) and Hoagland's solutions with 150 mM NaCl (salt treatment) to culture in a growth room. The roots from L2010-3 and BML1234 were separately collected at 0 h (control), 6 h (control, treatment), 18 h (control, treatment), and 36 h (control, treatment) with two biological replicates, and a total of 28 samples were subjected to transcriptome sequencing. The obtained raw sequencing reads were filtered by fastp software and the

clean reads were retained. Gene expression levels were calculated by the clean reads mapped on B73 genome and were then normalized to transcripts per kilobase million (TPM) via consumer script. The TPM of candidate genes detected by GWAS were subjected to WGCNA based on the WGCNA package in R studio software (Langfelder and Horvath, 2008). The parameters of WGCNA program were as follows: variance data expression > 0; no missing data expression < 0.1; soft threshold = 8 (estimate value); max block size = 200; deep split = 2; min module size = 3; merge cut height = 0.1. In each module, the genes with eigengene-based connectivity value (|KME|) > 0.9 and topological overlap measure (TOM) value > 0.2 were regarded as hub genes (Buckberry et al. 2017; Zhang and Horvath, 2005). Function annotations of the candidate genes were obtained by searching NCBI website (RefGen_v2) (https://www.ncbi.nlm.nih.gov/). Kyoto encyclopedia of genes and genomes (KEGG) pathway analyses were implemented in GENE DENOVO platform (https://www.omicshare.com/tools/Home/Soft/pathwaygsea). Cytoscape software was used to draw the regulation networks of target genes (Shannon et al. 2003).

Candidate gene association study

Among these hub genes, the ones that were reported to correlate with salt tolerance of plant species were considered as prioritized hub genes and were individually subjected to candidate gene association study. The gene body and its upstream 2,000 bp sequences were PCR-amplified in 77 randomly selected inbred lines from the association panel. Primers were designed in Primer 3.0 (v. 0.4.0). DNAMAN software (version5.2.2, lynnon bio-soft, Canada) was used to perform sequence alignment between the amplified sequences and B73 genome sequence to identify sequence diversity including SNPs and insertion/deletion (InDels) (Zhang et al. 2020b). The associations between the phenotypes and SNPs/InDels with MAF ≥ 0.05 were analyzed by conducting candidate gene association based on a GLM + PCA model in TASSEL 4.0 software with the significant threshold P = 0.01 (Bradbury et al. 2007). LD decay between the SNPs was calculated by HaploView software (http://www.broad.mit.edu/mpg/haploview). Haplotypes were identified by using significant markers located in target genes.

Superior allele analysis in elite lines

For each significant SNP detected in SS conditions, a superior allele was determined by the effect value. For each SNP, the superior allele proportion was equal to the number of superior alleles in the elite lines divided by the total alleles in the elite lines (Ma et al., 2018). Additionally, the heatmap of superior allele distributions was drawn in the R software using a heatmap package.

Results

Evaluation of salt-tolerance phenotypes

To systematically evaluate the phenotypes of salt-tolerance, mean value, standard deviation (SD), maximum value, and minimum value were collected for each trait. For all traits, highly phenotypic

variations were observed with SDs ranged from 0.12 to 937.81 (Table S1). Significant differences (P < 0.001) for all traits were detected between NT and SS (Fig. 1), suggesting salt stress in the association panel was effective. Under SS conditions, SNaC, RNaC, SNaC/SKC, RNaC/RKC, and KTC were obviously enhanced with the increased folds ranged from 0.54 to 18.32, whereas SKC, RKC, and NaTC were greatly lowered with the decreased folds ranged from 0.26 to 0.52 in comparison to their corresponding phenotypes under NT condition (Fig. 1; Table S1). Under NT and SS conditions, the phenotype frequency distributions of all traits displayed normal distributions (Fig. 1). Broad-sense heritability (H_B^2) estimates of traits were in a range of 0.35-0.89 across two conditions (Table S1). Under NT condition, SNaC and SNaC/SKC displayed the highest positive correlation (r = 0.88), whereas RKC and KTC showed the highest negative correlation (r = -0.65) (Table S2). Under SS condition, the highest positive correlation was observed between NaTC and SNaC, with r = 0.80, and the highest negative correlation was observed between SNaC and SNaC/SKC, with r = -0.63 (Table S2).

GWAS

Using FarmCPU model, two and seven significant SNPs were detected under NT and SS conditions, respectively, at a P-value threshold of 1.08×10^{-6} (Fig. 2; Table S3). In NT condition, PZE-101252072 and SYN33050 were associated with RNaC (P = 2.95×10^{-7}, SNP effect = -25.64; P = 3.15×10^{-7}, SNP effect = -25.24) (Fig. 2a; Table S3). In SS condition, four SNaC/SKC-associated significant SNPs, namely SYN38412, PZE-104132392, SYN6394, and PZE-110042260 were detected by FarmCPU model with the P values of 1.09×10^{-7}, 6.90×10^{-9}, 1.76×10^{-7}, and 9.44×10^{-8}, respectively (Fig. 2b; Table S3). The SNPs SYN24195 and PUT-163a-21390620-1531 controlling KTC were separately identified on chromosomes 1 and 2 (P = 2.33×10^{-7}, SNP effect = 0.89; P = 1.25×10^{-7}, SNP effect = -1.05), and SYN26336 controlling RKC was identified on chromosome 9 (P = 5.28×10^{-7}, SNP effect = -98.44) (Fig. 2b; Table S3). Among the seven significant SNPs, four (SYN24195, SYN38412, SYN6394, and SYN26336) were located within the QTL (or LD regions of QTL) for salt stress response identified in previous studies (Table 1). According to the whole-genome LD decay distance (300 Kb), 44 and 120 candidate genes were respectively obtained in NT and SS conditions, of which no genes were simultaneously detected under both conditions (Table S4). Among the 120 candidate genes detected in SS conditions, six genes *GRMZM2G104783*, *GRMZM2G372952*, *GRMZM2G372632*, *GRMZM2G171428*, *GRMZM2G378852*, and *GRMZM2G070304* were associated with salt stress based on the functions of their homologues in plants (Table S4). Collectively, all these findings verified the credibility of the genetic loci detected by our GWAS.

WGCNA

To further identify the hub genes out of all 120 candidate genes from GWAS, we conducted a WGCNA using the expression values (TPM) of these genes. As a result, these 120 genes were classed into four subgroups, namely blue, brown, turquoise, and yellow modules (Fig. 3a). Kyoto encyclopedia of genes and genomes (KEGG) pathway analysis revealed that the genes in the blue, brown, and turquoise modules were significantly (P < 0.05) enriched in five (glucosinolate biosynthesis, valine, leucine and isoleucine biosynthesis, pantothenate and CoA biosynthesis, ribosome, and valine, leucine and isoleucine

degradation), two (RNA transport, and protein processing in endoplasmic reticulum), one (ABC transporters) pathways, respectively. As for the yellow module, no significant pathway was enriched. Additionally, a total of nine genes were discovered and subsequently defined as hub genes with the principles of |KME| > 0.9 and TOM > 0.2 (Table 2), of which one (*GRMZM2G061830*, KME = 0.95, TOM = 0.24), five (*AC206223.3_FG004*, KME = 0.97, TOM = 0.24; *GRMZM2G075104*, KME = -0.92, TOM = 0.33; *GRMZM2G096622*, KME = 0.91, TOM = 0.33; *GRMZM2G333183*, KME = -0.95, TOM = 0.45; and *GRMZM2G502467*, KME = -0.94, TOM = 0.37), and three (*GRMZM2G066950*, KME = 0.93, TOM = 0.55; *GRMZM2G066840*, KME = 0.92, TOM = 0.20; *GRMZM2G308463*, KME = 0.96, TOM = 0.53) existed in blue, turquoise, and yellow modules, respectively (Table 2). Most strikingly, ABC transporters were previously reported to be key factors in regulating ion exchange under salt stress, therefore, turquoise module was focused in our study (Moons, 2003; Saha et al. 2015). In turquoise module, *GRMZM2G075104* and *GRMZM2G333183* respectively annotated as ubiquitin conjugation factor E4 and ABC transporter B family member 14 (Table 2), which participates in salt stress response in Spinach (*Spinacia oleracea L.*), *Arabidopsis*, *Oryza sativa* and other species (Bagheri et al. 2015; Lee and Kim 2011; Moons 2003; Saha et al. 2015). As such, *GRMZM2G075104* and *GRMZM2G333183* were considered as prioritized hub genes for further study. According to the node cytoscape results from WGCNA, we constructed the regulation networks of the genes located in turquoise module (Fig. 3b).

Candidate gene association analysis

To excavate the intragenic loci affecting the phenotypic values and identify the favorable haplotype, we performed PCR-amplifications for the gene regions and promoters (upstream: 2,000 bp) of two prioritized hub genes *GRMZM2G075104* and *GRMZM2G333183*respectively. The results showed that 42 (1 InDel and 41 SNPs) and 45 (1 InDel and 44 SNPs) variation loci with MAF ≥ 0.05 existed in *GRMZM2G075104* and *GRMZM2G333183*, respectively. Association analyses using GLM + PCA model indicated that 10 significant markers (one Indel and nine SNPs) were associated with SNaC/SKC and SKC for *GRMZM2G075104* (Fig. 4a). Among them, SNP S9_126198762 (P = 3.91 × 10^{-3}) was a missense variant (C/T) which located in the third exon and the remaining nine loci (P = 3.39-8.90 × 10^{-3}) were intron variants (Fig. 4a). For *GRMZM2G333183*, three significant SNPs were found (Fig. 5a), among which S10_79997882 (C/T, P = 7.56 × 10^{-5}) and S10_79998205 (T/C, P = 5.62 × 10^{-4}) were both located in the promoter region and were associated with RKC and RNa/RKC, respectively (Fig. 5a). In addition, an Indel S10_79996578 (CCTT/T) associated with RNa/RKC (P = 8.19 × 10^{-5}) resided in the intron region of *GRMZM2G333183* (Fig. 5a). The pairwise LD of polymorphisms were also separately calculated via HaploView software for the two genes (Fig. 4b, Fig. 5b). In *GRMZM2G075104*, seven significant variants, S9_126194850, S9_126197102, S9_126197408, S9_126197482, S9_126198762, S9_126199321, and S9_126200226 located within a block, the remaining three markers S9_126202855, S9_126202900, and S9_126203065 occurred in another block (Fig. 4b).

Among all the haplotypes identified in each of *GRMZM2G075104* and *GRMZM2G333183*, a haplotype with lower SNaC/SKC (RNaC/RKC) or higher SKC (RKC) was designated as a favorable/tolerant haplotype. For *GRMZM2G075104*, two haplotype groups (Hap I and Hap II) were obtained according to

the significant markers (Fig. 4e). Compared with Hap I (CCAATTTGTC), Hap II (TTGTCCG-CT) showed significantly higher (P = 0.022) SKC and lower (P = 0.004) SNaC/SKC, therefore Hap II was considered as the favorable haplotype (Fig. 4c, d). Meanwhile, based on the significant loci in *GRMZM2G333183*, these 77 lines were divided into three haplotypes, Hap III (CTT) had significantly higher RKC (P = 0.007) and lower SNaC/SKC (P = 0.006) than Hap I (-TC), thus Hap III was confirmed as the favorable allele (Fig. 5c-e).

Distribution of superior alleles in elite inbred lines

Since our association panel included 30 elite lines which were collected from maize breeding programs (Ma et al. 2018), this allowed us to estimate the utilization of superior alleles during maize breeding. According to the GWAS results, significant SNPs were detected for SNaC/SKC, RKC, and KTC under salt stress condition. Herein, the allele associated with a lower phenotype was defined as the superior allele for SNaC/SKC, whereas the allele with a higher phenotype was designated as the superior allele for RKC and KTC. Among the 30 elite inbred lines, the superior allele percentages of significant SNPs ranged from 10.71% to 93.00%, with five of SNPs (SYN38412, PZE-104132392, SYN6394, PZE-110042260, and SYN24195) containing $\geq$ 50% superior alleles whereas the remaining two SNPs (SYN26336 and PUT-163a-21390620-1531) containing < 50% superior alleles (Fig. 6). Moreover, 20 elite lines that contained 4-7 superior alleles displayed higher phenotypic values, with increased percentages of 22.92% (RKC), and 65.91% (KTC), relative to the other 10 elite lines that contained 0-3 superior alleles. However, for SNaC/SKC, the above 20 lines that contained 4-7 superior alleles had a lower mean value in comparison to the other 10 lines that contained 0-3 superior alleles, with the reduced percentage of 55.52%. These findings suggested that the superior alleles have obviously additive effects on salt tolerance.

Discussion

Using Na$^+$ and K$^+$-related traits for evaluating salt tolerance in maize

In previous studies, seedling shoot length, root length, shoot fresh weight, root fresh weight, shoot dry weight, root dry weight, tissue water content, plant height, and plant survival rate were used to evaluate the salt tolerance in maize (Cui et al. 2015; Luo et al. 2017; Luo et al. 2019a; Luo et al. 2019b). According to the genetic architecture analysis of these traits, several QTL controlling maize salt tolerance were identified. However, all these traits represent indirect responses to salt stress. Under salt stress, Na$^+$ and K$^+$-related traits (SNaC, RNaC, SKC, RKC, SNaC/SKC, RNaC/RKC, KTC, and NaTC) are direct evaluation standards for salt tolerance of plants. Meanwhile, these traits are involved in two salt-plant signals, SOS and HKT pathways. Recently, two Na$^+$ and K$^+$ transporter *HKT1* and *HAK4* were demonstrated to mediate salt tolerance of maize under salinity conditions (Zhang et al. 2018; Zhang et al. 2019). Therefore, Na$^+$ and K$^+$-related traits were taken as evaluation indexes for salt tolerance of maize seedlings in this study. Abundant phenotypic variations were observed for all measured traits in this association panel, with the variation coefficients of 24.01-50.00% and 27.21-89.24% in NT and SS, respectively (Table S1), suggesting this panel was suitable for GWAS of the eight Na$^+$ and K$^+$-related traits under two conditions.

A combination of GWAS and WGCNA is an efficient strategy for elucidating genetic architecture and hub genes of salt tolerance in maize

Currently, GWAS is widely used in dissecting genetic basis of complex agronomic traits. Using GWAS, previous studies revealed many candidate genes controlling target traits in maize. For embryonic callus regenerative capacity in maize, a total of 40 candidate genes were identified using GWAS, including a previously verified gene *WOX2* (Ma et al. 2018). Zhang et al. (2020a) found an ear row number-associated SNP SYN8062 in an association panel, which was closely linked to the gene model *GRMZM2G098557*. Subsequently, *GRMZM2G098557* was validated to regulate ear row number by using a segregation population. Similarly, several genes associated with salt tolerance were also detected by GWAS in maize, such as *HKT1* and *HAK4* (Zhang et al. 2018; Zhang et al. 2019). Herein, according to the GWAS results, several candidate genes were associated with salt tolerance of maize seedlings. Among them, *GRMZM2G104783* (PZE-104132392), involved in SNaC/SKC was annotated as a cytochrome P450 superfamily protein (Table S4). In *Arabidopsis thaliana*, a *cyp709b3* (a member of cytochrome P450 superfamily) mutant showed sensitivity to salt during germination and low tolerance to salt stress (NaCl concentration: 150 mM) (Mao et al. 2013). In *Gossypium hirsutum*, two cytochrome P450 members, *Gh_D07G1197* and *Gh_A13G2057* played positive roles in enhancing drought and salt stress tolerance (Magwanga et al. 2019). A SNaC/SKC-associated gene, *GRMZM2G372952* (SYN6394) was annotated as a zinc finger protein ZAT4 (Table S4). Sun et al. (2019) reported that the salt and drought tolerances were enhanced by overexpressing the *GMZAT4* in *Arabidopsis thaliana*. The SNaC/SKC-correlated gene *GRMZM2G372632* (SYN6394) encodes a pentatricopeptide repeat-containing protein At4g31850 in chloroplastic (Table S4), the homologous gene of which, *wsl* was reported to enhance salinity sensitivity in rice (Tan et al. 2014). *GRMZM2G171428* (SYN6394) that was associated with SNaC/SKC encodes a WRKY transcription factor 4 (Table S4). Previous studies showed that a WRKY transcription factor *WRKY17* negatively regulated salt stress tolerance in transgenic *Nicotiana benthamiana* and *Arabidopsis* via abscisic acid signaling pathway (Yan et al. 2014; Cai et al. 2017). However, overexpression of another WRKY transcription factor *VvWRKY30* in *Arabidopsis* increased its resistance to salt stress at different growth stages (Zhu et al. 2019). A RKC-associated gene *GRMZM2G378852* (SYN26336) encodes a MAPKKK family protein kinase (Table S4), whose homologous gene, *At1g73660* was demonstrated to negatively regulate the salt tolerance in *Arabidopsis* (Gao and Xiang 2008). Gene model *GRMZM2G070304* (PUT-163a-21390620-1531) that was involved in KTC was annotated as glycerol-3-phosphate acyltransferase 3 (*GPAT3*) (Table S4). Sui et al. (2017) confirmed that the salt tolerance of *Arabidopsis* could be improved by overexpressing the homologous gene (*SsGPAT*) of *GRMZM2G070304* from *Suaeda salsa*. Moreover, two genes *GRMZM2G075104* and *GRMZM2G333183*, belonging to ubiquitin conjugation factor E4 and ABC transporter B family member 14, respectively (Table S4), were reported to be associated with salt stress tolerance in Spinach (*Spinacia oleracea L.*), *Arabidopsis*, *Oryza sativa* and other species (Bagheri et al. 2015; Lee and Kim 2011; Moons 2003; Saha et al. 2015).

Recently, to decode the genetic control and hub candidate genes related to target traits, a joint analysis of GWAS and WGCNA has become an efficient approach. Using this strategy, two hub genes *GRMZM2G477685* and *GRMZM2G135536* controlling primary root growth were identified by Hwang et al.

(2018). Similarly, Guo et al. (2020) detected seven hub candidate genes involved in seminal root length of maize seedlings under drought stress though GWAS and WGCNA. In our study, we totally identified nine candidate genes associated with salt tolerance in maize seedlings by using a combination of GWAS and WGCNA (Table 2). Combined with the gene annotations, *GRMZM2G075104* and *GRMZM2G333183* were finally determined as hub genes. Therefore, these two promising genes were prioritized for further study.

Interaction predictions of hub genes

In this study, the hub genes *GRMZM2G075104* and *GRMZM2G333183* were both located in turquoise module. To identify the upstream regulators of the two hub genes, we further focused on these transcript factors in turquoise module. Among the 19 genes co-expressed with *GRMZM2G333183* (Fig.3b), only *GRMZM2G171428* was annotated as transcript factor (WRKY transcription factor 4) in this module. Interestingly, we found a WRKY binding motif (TAGTCAAA) in the promoter region (upstream 3,000 bp) of *GRMZM2G333183* (P value = 9.62E-05) using the plant transcriptional regulatory map website (http://plantregmap.gao-lab.org/index.php). This finding suggested that the WRKY transcription factor, *GRMZM2G171428* probably regulate the hub gene *GRMZM2G333183* by binding the motif (TAGTCAAA) in the promoter of *GRMZM2G333183*. Utilizing STRING software (https://string-db.org/), we subsequently predicted the encoding protein interactions between the hub genes and the other genes in the co-expression network. Eventually, we didn't search out any interaction in turquoise module for hub genes *GRMZM2G075104* and *GRMZM2G333183*, indicating the encoding proteins of hub genes performed functions independently.

Identification of superior haplotypes for hub genes

Currently, traditional breeding methods in crops produce lower genetic gains than required to achieve food sufficiency. In this context, advanced breeding technologies should be proposed and utilized. Superior haplotypes affecting many agronomic traits (such as yield, kernel quality, and abiotic stress responsiveness etc.) have been verified across maize (Yu et al. 2019; Li et al. 2020; Zhang et al. 2020b). Genetic variations occurred in promoter and coding regions probably leads to the variations of gene expression abundances and protein sequences. Candidate gene association analysis was able to identify the significant variations based on a P-value threshold and thus widely used in detecting/dividing superior haplotypes of target genes. Using this method, Li et al. (2020) analyzed the haplotypes of candidate genes associated with trait ear tip-barrenness in maize. Zhang et al. (2020b) reported one favorable haplotype for gene *Zm00001d047868* which influenced maize kernel moisture content. Additionally, a previous study reported that overexpressing favorable haplotype of *ZmEREB180* increased maize waterlogging tolerance (Yu et al. 2019). In this study, the favorable haplotypes of *GRMZM2G075104* and *GRMZM2G333183* were determined as TTGTCCG-CT and CTT using candidate gene association analysis, respectively. In future studies, to verify the functions of *GRMZM2G075104* and *GRMZM2G333183*, the favorable haplotypes TTGTCCG-CT and CTT should be given priority for overexpression/knockout. In addition, superior haplotypes TTGTCCG-CT and CTT identified in this study can be used for molecular marker-assisted breeding of increasing salt tolerance in maize.

Application of superior alleles in cultivating salt-tolerance maize varieties

According to the distributions of seven significant SNPs uncovered in 30 elite inbred lines, we found two SNPs (SYN26336 and PUT-163a-21390620-1531) containing < 50% superior alleles (Fig. 6), which suggested that these alleles were not effectively selected during artificial selections. The possible reason is that maize salt tolerance was not a main trait concerned by breeders. The other five SNPs (SYN38412, PZE-104132392, SYN6394, PZE-110042260, and SYN24195) contained ≥ 50% superior alleles across the 30 elite lines (Fig. 6). Especially for PZE-104132392 and PZE-110042260, 27 superior alleles (90%) were observed among the 30 elite lines (Fig. 6). These findings implied that these alleles might linked with some major traits and were simultaneously maintained with the concerned traits in breeding programs. In further studies, the SNPs with low proportions of superior alleles should be emphasized by marker-assisted selection in cultivating salt-tolerance maize varieties. In addition, the inbred lines K22 and F06 contained seven (100%) and six (85.7%) superior alleles, respectively (Fig. 6), indicating these were salt-tolerance lines. The present findings implied that K22 and F06 can be used for gene functional research of salt stress and breeding of salt-tolerance maize varieties.

Declarations

Author contributions

YS and LM designed the experiment. LM, MZ, JC, CQ, SH, CZ, GY, CY and HP collected the phenotypes and performed the data analysis. LM and YS wrote the manuscript. LM, YS, GP and TL edited this draft. All authors have read and approved the manuscript.

Acknowledgments

Compliance with ethical standards

Conflict of interest

The authors declare that the research was conducted in the absence of any commercial or financial relationship that could be construed as a potential conflict of interest.

Human and animal rights

This study does not include human or animal subjects.

Availability of data and materials

All raw data generated of 28 samples used in this study were deposited in Genome Sequence Archive (GSA) in National Genomics Data Center (NGDC) database with the accession number CRA003872.

References

Bagheri R, Bashir H, Ahmad J, Iqbal M, Qureshi MI (2015) Spinach (*Spinacia oleracea* L.) modulates its proteome differentially in response to salinity, cadmium and their combination stress. Plant Physiol Biochem 97: 235–245

Bradbury PJ, Zhang Z, Kroon DE, Casstevens TM, Ramdoss Y, Buckler ES (2007) TASSEL: software for association mapping of complex traits in diverse samples. Bioinformatics 23(19): 2633–2635

Buckberry S, Bianco-Miotto T, Bent SJ, Clifton V, Shoubridge C, Shankar K, Roberts CT (2017) Placental transcriptome co-expression analysis reveals conserved regulatory programs across gestation. BMC Genomics 18(1): 1–13

Cai R, Dai W, Zhang C, Wang Y, Wu M, Zhao Y, Ma Q, Xiang Y, Cheng B (2017) The maize WRKY transcription factor ZmWRKY17 negatively regulates salt stress tolerance in transgenic *Arabidopsis* plants. Planta, 246(6): 1215–1231

Cui D, Wu D, Somarathna Y, Xu X, Li S, Li P, Zhang H, Chen H, Zhao L (2015) QTL mapping for salt tolerance based on snp markers at the seedling stage in maize (*Zea mays* L.). Euphytica 203(2): 273–283

Gao L, Xiang CB (2008). The genetic locus At1g73660 encodes a putative MAPKKK and negatively regulates salt tolerance in *Arabidopsis*. Plant Mol Biol 67(1): 125–134

Guo J, Li C, Zhang X, Li Y, Zhang D, Shi Y, Song Y, Li Y, Yang D, Wang T (2020) Transcriptome and GWAS analyses reveal candidate gene for seminal root length of maize seedlings under drought stress. Plant Sci 292: 110380

Halfter U, Ishitani M, Zhu JK (2000) The *Arabidopsis* SOS2 protein kinase physically interacts with and is activated by the calcium-binding protein SOS3. Proc Natl Acad Sci USA 97(7): 3735–3740

Hamamoto S, Horie T, Hauser F, Deinlein U, Schroeder JI, Uozumi N (2015) HKT transporters mediate salt stress resistance in plants: from structure and function to the field. Curr Opin Biotechnol 32: 113–120

Hamwieh A, Xu D (2008) Conserved salt tolerance quantitative trait locus (QTL) in wild and cultivated soybeans. Breed Sci 58(4): 355–359

Hazzouri KM, Khraiwesh B, Amiri KMA, Pauli D, Blake T, Shahid M, Mullath SK, Nelson D, Mansour AL, Salehi-Ashtiani K, Purugganan M, Masmoudi K (2018) Mapping of *HKT1; 5* gene in barley using GWAS approach and its implication in salt tolerance mechanism. Front Plant Sci 9: 156

Hoque MMI (2013). Evaluation and mapping QTLs of maize salinity tolerance. Dissertation, Chinese Academy of Agricultural Sciences

Hu S, Sanchez DL, Wang C, Lipka AE, Yin Y, Gardner CAC, Lübberstedt T (2017) Brassinosteroid and gibberellin control of seedling traits in maize (*Zea mays* L.). Plant Sci 263: 132–141

Hu Y, Schmidhalter U (2005) Drought and salinity: a comparison of their effects on mineral nutrition of plants. J Plant Nutr Soil Sci 168(4): 541–549

Hwang SG, Kim KH, Lee BM, Moon JC (2018) Transcriptome analysis for identifying possible gene regulations during maize root emergence and formation at the initial growth stage. Genes Genom 40(7): 755–766

Ji H, Pardo JM, Batelli G, Van Oosten MJ, Bressan RA, Li X (2013) The salt overly sensitive (SOS) pathway: established and emerging roles. Mol Plant 6(2): 275–286

Korte A, Farlow A (2013) The advantages and limitations of trait analysis with GWAS: a review. Plant Methods 9(1): 1–9

Kumar V, Singh A, Mithra SVA, Krishnamurthy SL, Parida SK, Jain S, Tiwari KK, Kumar P, Rao AR, Sharma SK, Khurana JP, Singh NK, Mohapatra T (2015) Genome-wide association mapping of salinity tolerance in rice (*Oryza sativa*). DNA Res 22(2): 133–145

Langfelder P, Horvath S (2008) WGCNA: an R package for weighted correlation network analysis. BMC Bioinformatics 9(1): 1–13

Lee JH, Kim WT (2011) Regulation of abiotic stress signal transduction by E3 ubiquitin ligases in *Arabidopsis*. Mol Cells 31(3): 201–208

Lipka AE, Tian F, Wang Q, Peiffer J, Li M, Bradbury PJ, Gore MA, Buckler ES, Zhang Z (2012) GAPIT: genome association and prediction integrated tool. Bioinformatics 28: 2397–2399

Liu J, Ishitani M, Halfter U, Kim CS, Zhu JK (2000) The *Arabidopsis thaliana SOS2* gene encodes a protein kinase that is required for salt tolerance. Proc Natl Acad Sci USA 97(7): 3730–3734

Liu X, Huang M, Fan B, Buckler ES, Zhang Z (2016b) Iterative usage of fixed and random effect models for powerful and efficient genome-wide association studies. PLoS Genet 12: e1005767

Liu Y, Xie S, Yu J (2016a) Genome-wide analysis of the lysine biosynthesis pathway network during maize seed development. PLoS One 11(2): e0148287

Li Z, Liu P, Zhang X, Zhang Y, Ma L, Liu M, Guan Z, Zhang Y, Li P, Zou C, He Y, Gao S, Pan G, Shen Y (2020) Genome-wide association studies and QTL mapping uncover the genetic architecture of ear tip-barrenness in maize. Physiol Plant 170(1): 27–39

Luo M, Zhang Y, Chen K, Kong M, Song W, Lu B, Shi Y, Zhao Y, Zhao J (2019a) Mapping of quantitative trait loci for seedling salt tolerance in maize. Mol Breed 39(5): 1–12

Luo M, Zhao Y, Zhang R, Xing J, Duan M, Li J, Wang N, Wang W, Zhang S, Chen Z, Zhang H, Shi Z, Song W, Zhao J (2017) Mapping of a major QTL for salt tolerance of mature field-grown maize plants based on SNP markers. BMC Plant Biol 17(1): 1–10

Luo X, Wang B, Gao S, Zhang F, Terzaghi W, Dai M (2019b) Genome-wide association study dissects the genetic bases of salt tolerance in maize seedlings. J Integr Plant Biol 61(6): 658–674

Magwanga RO, Lu P, Kirungu JN, Dong Q, Cai X, Zhou Z, Wang X, Hou Y, Xu Y, Peng R, Agong SG, Wang K, Fang L (2019) Knockdown of cytochrome P450 genes *Gh_D07G1197* and *Gh_A13G2057* on chromosomes D07 and A13 reveals their putative role in enhancing drought and salt stress tolerance in *Gossypium hirsutum*. Genes 10(3): 226

Ma L, Liu M, Yan Y, Qing C, Zhang X, Zhang Y, Long Y, Wang L, Pan L, Zou C, Li Z, Wang Y, Peng H, Pan G, Jiang Z, Shen Y (2018) Genetic dissection of maize embryonic callus regenerative capacity using multi-locus genome-wide association studies. Front Plant Sci 9: 561

Ma L, Qing C, Frei U, Shen Y, Lübberstedt T (2020) Association mapping for root system architecture traits under two nitrogen conditions in germplasm enhancement of maize doubled haploid lines. Crop J 8(2): 213–226

Mao G, Seebeck T, Schrenker D, Yu O (2013) CYP709B3, a cytochrome P450 monooxygenase gene involved in salt tolerance in *Arabidopsis thaliana*. BMC Plant Biol 13(1): 1–13

Moons A (2003) *Ospdr9*, which encodes a PDR-type ABC transporter, is induced by heavy metals, hypoxic stress and redox perturbations in rice roots. FEBS Lett 553(3): 370–376

Munns R (2002) Comparative physiology of salt and water stress. Plant Cell Environ 25(2): 239–250

Pace J, Gardner C, Romay C, Ganapathysubramanian B, Lübberstedt T (2015) Genome-wide association analysis of seedling root development in maize (*Zea mays* L.). BMC Genomics 16(1): 1–12

Quintero FJ, Martinez-Atienza J, Villalta I, Jiang X, Kim WY, Ali Z, Fujii H, Mendoza I, Yun DJ, Zhu JK, Pardo JM (2011) Activation of the plasma membrane Na^+/H^+ antiporter salt-overly-sensitive 1 (SOS1) by phosphorylation of an auto-inhibitory C-terminal domain. Proc Natl Acad Sci USA 108(6): 2611–2616

Ren ZH, Gao JP, Li LG, Cai XL, Huang W, Chao DY, Zhu MZ, Wang ZY, Luan S, Li HX (2005) A rice quantitative trait locus for salt tolerance encodes a sodium transporter. Nature Genet 37(10): 1141–1146

Ryu H, Cho YG (2015) Plant hormones in salt stress tolerance. J Plant Biol 58(3): 147–155

Saha J, Sengupta A, Gupta K, Gupta B (2015) Molecular phylogenetic study and expression analysis of ATP-binding cassette transporter gene family in *Oryza sativa* in response to salt stress. Comput Biol Chem 54: 18–32

Schaefer RJ, Michno JM, Jeffers J, Hoekenga O, Dilkes B, Baxter I, Myers CL (2018) Integrating co-expression networks with GWAS to prioritize causal genes in maize. Plant Cell 30(12): 2922–2942

Shannon P, Markiel A, Ozier O, Baliga NS, Wang JT, Ramage D, Amin N, Schwikowski B, Ideker T (2003) Cytoscape: a software environment for integrated models of biomolecular interaction networks. Genome Res 13(11): 2498–2504

Shi H, Ishitani M, Kim C, Zhu JK (2000) The Arabidopsis thaliana salt tolerance gene *SOS1* encodes a putative Na^+/H^+ antiporter. Proc Natl Acad Sci USA 97(12): 6896–6901

Shi H, Quintero FJ, Pardo JM, Zhu JK (2002) The putative plasma membrane Na^+/H^+ antiporter *SOS1* controls long-distance Na^+ transport in plants. Plant Cell 14(2): 465–477

Sui N, Tian S, Wang W, Wang M, Fan H (2017) Overexpression of glycerol-3-phosphate acyltransferase from *Suaeda salsa* improves salt tolerance in *Arabidopsis*. Front Plant Sci 8: 1337

Sukumaran S, Dreisigacker S, Lopes M, Chavez P, Reynolds MP (2015) Genome-wide association study for grain yield and related traits in an elite spring wheat population grown in temperate irrigated environments. Theor Appl Genet 128(2): 353–363

Sun Z, Liu R, Guo B, Huang K, Wang L, Han Y, Li H, Hou S (2019) Ectopic expression of GmZAT4, a putative C2H2-type zinc finger protein, enhances PEG and NaCl stress tolerances in *Arabidopsis thaliana*. 3 Biotech 9(5): 166

Tan J, Tan Z, Wu F, Sheng P, Heng Y, Wang X, Ren Y, Wang J, Guo X, Zhang X, Cheng Z, Jiang L, Liu X, Wang H, Wan J (2014) A novel chloroplast-localized pentatricopeptide repeat protein involved in splicing affects chloroplast development and abiotic stress response in rice. Mol Plant 7(8): 1329–1349

Wang ZF, Wang JF, Bao YM, Wu YY, Zhang HS (2011) Quantitative trait loci controlling rice seed germination under salt stress. Euphytica 178(3):297–307

Wan Q, Tang J, Han Y, Wang D (2018) Co-expression modules construction by WGCNA and identify potential prognostic markers of uveal melanoma. Exp Eye Res 166: 13–20

Yan H, Jia H, Chen X, Hao L, An H, Guo X (2014) The cotton WRKY transcription factor GhWRKY17 functions in drought and salt stress in transgenic *Nicotiana benthamiana* through ABA signaling and the modulation of reactive oxygen species production. Plant Cell Physiol 55(12): 2060–2076

Yu F, Liang K, Fang T, Zhao H, Han X, Cai M, Qiu F (2019) A group VII ethylene response factor gene, *ZmEREB180*, coordinates waterlogging tolerance in maize seedlings. Plant Biotechnol J 17(12): 2286–2298

Zhang B, Horvath S (2005) A general framework for weighted gene co-expression network analysis. Stat Appl Genet Mol Biol 4(1)

Zhang M, Cao Y, Wang Z, Wang ZQ, Shi J, Liang X, Song W, Chen Q, Lai J, Jiang C (2018) A retrotransposon in an HKT1 family sodium transporter causes variation of leaf Na$^+$ exclusion and salt tolerance in maize. New Phytol 217(3): 1161–1176

Zhang M, Liang X, Wang L, Gao Y, Song W, Shi J, Lai J, Jiang C (2019) A HAK family Na$^+$ transporter confers natural variation of salt tolerance in maize. Nat Plants 5(12): 1297–1308

Zhang X, Guan Z, Li Z, Liu P, Ma L, Zhang Y, Pan L, He S, Zhang Y, Li P, Ge F, Zou C, He Y, Gao S, Pan G, Shen Y (2020a) A combination of linkage mapping and GWAS brings new elements on the genetic basis of yield-related traits in maize across multiple environments. Theor Appl Genet 133(10): 2881–2895

Zhang X, Liu P, Qing C, Yang C, Shen Y, Ma L (2021) Comparative transcriptome analyses of maize seedling root responses to salt stress. PeerJ 9: e10765

Zhang X, Zhang H, Li L, Lan H, Ren Z, Liu D, Wu L, Jaqueth J, Li B, Pan G, Gao S (2016) Characterizing the population structure and genetic diversity of maize breeding germplasm in Southwest China using genome-wide SNP markers. BMC Genomics 17(1): 1-16

Zhang Y, Hu Y, Guan Z, Liu P, He Y, Zou C, Li P, Gao S, Peng H, Yang C, Pan G, Shen Y, Ma L (2020b) Combined linkage mapping and association analysis reveals genetic control of maize kernel moisture content. Physiol Plant 170(4): 508–518

Zhao X, Luo L, Cao Y, Liu Y, Li Y, Wu W, Lan Y, Jiang Y, Gao S, Zhang Z, Shen Y, Pan G, Lin H (2018) Genome-wide association analysis and QTL mapping reveal the genetic control of cadmium accumulation in maize leaf. BMC Genomics 19(1): 1–13

Zhu D, Hou L, Xiao P, Guo Y, Deyholos MK, Liu X (2019) *VvWRKY30*, a grape WRKY transcription factor, plays a positive regulatory role under salinity stress. Plant Sci 280: 132–142

Zhu JK (2001) Plant salt tolerance. Trends Plant Sci 6:66–71

Zhu JK (2002) Salt and drought stress signal transduction in plants. Annu Rev Plant Biol 53(1): 247–273

Tables

Table 1 Significant SNPs overlapping with QTL for salt stress response identified in previous studies.

SNP	Trait	Associated QTL	Distance between SNP and QTL (Mb)	Reference
SYN24195	KTC	*qSL*	—	Luo et al. 2019a
		qFL	—	Luo et al. 2019a
SYN38412	SNaC/SKC	*qPHI1* (SYN28626/PZE103019163)	0.13	Luo et al. 2017
SYN6394	SNaC/SKC	*qNPH9-2* (PZE109064469/SYN27201)	—	Luo et al. 2017
		qRF9	—	Luo et al. 2019a
		qSF9	—	Luo et al. 2019a
		qFF9	—	Luo et al. 2019a
		qRD9	—	Luo et al. 2019a
SYN26336	RKC	*qNPH9-2* (PZE109064469/SYN27201)	—	Luo et al. 2017

KTC, K$^+$ transport coefficient; SNaC/SKC, shoot Na$^+$ content/shoot K$^+$ content; RKC, root K$^+$ content.

"—" represents SNP located within the QTL.

Table 2 Details of hub genes detected by WGCNA.

Module	Gene	KME	TOM	Functional annotation
blue	*GRMZM2G061830*	0.95	0.24	NADH-cytochrome b5 reductase-like protein
turquoise	*AC206223.3_FG004*	0.97	0.24	Actin-interacting protein 1-2
turquoise	*GRMZM2G075104*	-0.92	0.33	Probable ubiquitin conjugation factor E4
turquoise	*GRMZM2G096622*	0.91	0.33	Ypt/Rab-GAP domain of gyp1p superfamily protein
turquoise	*GRMZM2G333183*	-0.95	0.45	ABC transporter B family member 14
turquoise	*GRMZM2G502467*	-0.94	0.37	—
yellow	*GRMZM2G066950*	0.93	0.55	—
yellow	*GRMZM2G066840*	0.92	0.20	Short-chain dehydrogenase reductase ATA1
yellow	*GRMZM2G308463*	0.96	0.53	Short-chain dehydrogenase reductase ATA1

WGCNA, KME and TOM represent weighted gene co-expression network analysis, eigengene-based connectivity value, and topological overlap measure value, respectively.

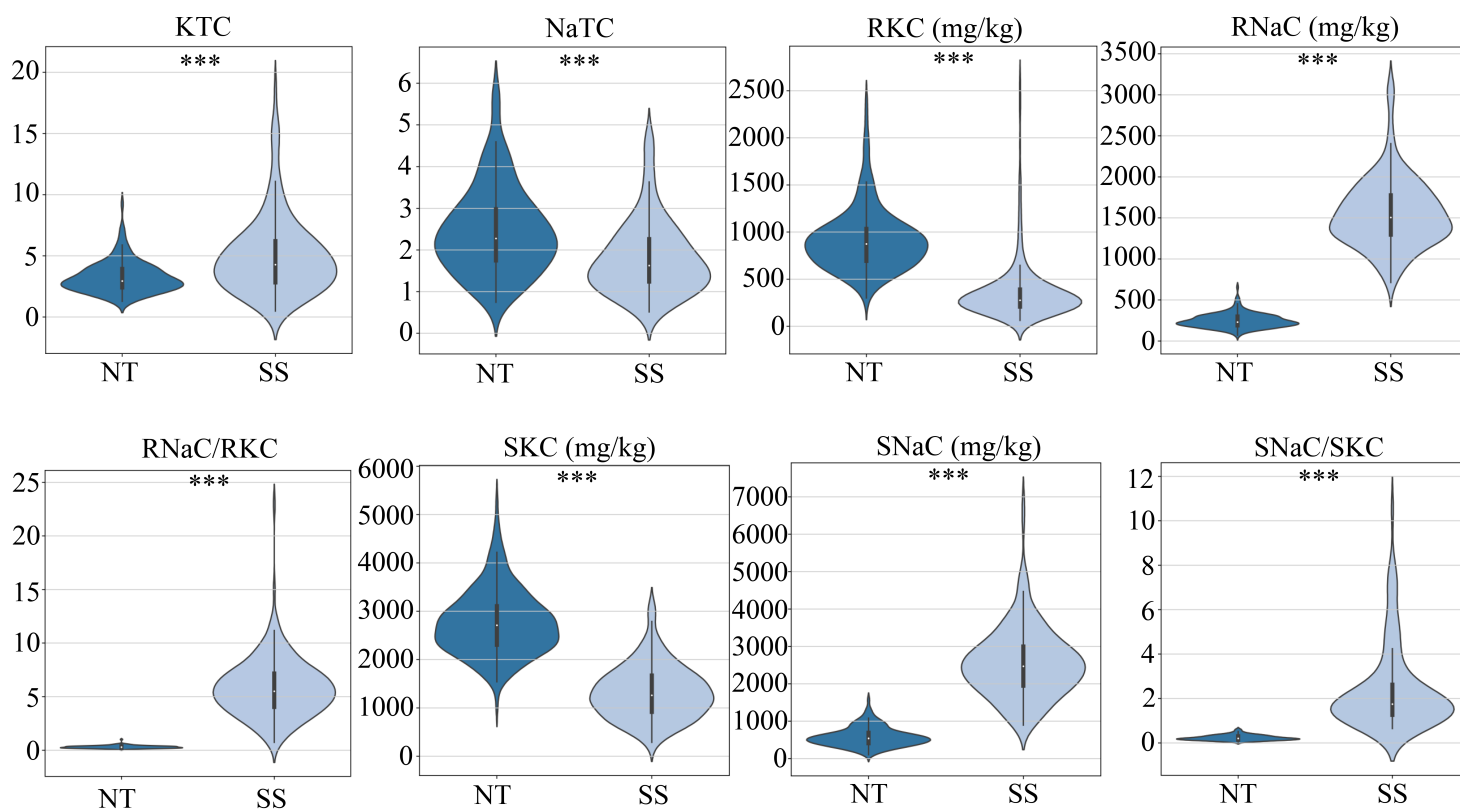"—" represents no functional annotations.

Figures

Figure 1

Phenotypes of the eight traits in NT and SS conditions. NT and SS represent normal treatment and salt stress, respectively. SNaC, shoot Na+ content; RNaC, root Na+ content; SKC, shoot K+ content; RKC, root K+ content; SNaC/SKC, shoot Na+ content/shoot K+ content; RNaC/RKC, root Na+ content/root K+ content; KTC, K+ transport coefficient; NaTC, Na+ transport coefficient. *** significant at P < 0.001.
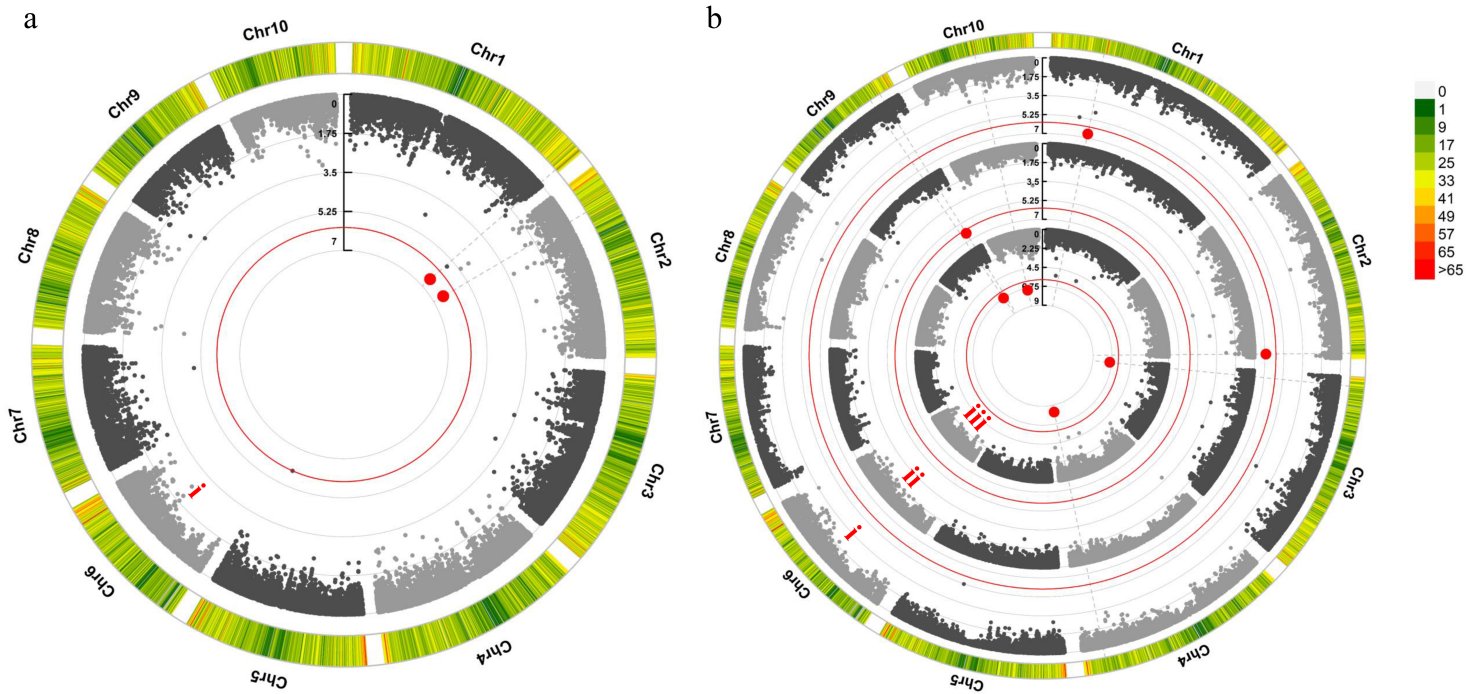

Figure 2

Significant SNPs detected in NT and SS conditions. (a) Significant SNPs detected in NT condition. NT represents normal treatment. Letter i represents trait RNaC (root Na+ content). Red dots represent significant SNPs associated with RNaC. (b) Significant SNPs detected in SS condition. SS represents salt stress. Letters i, ii, and iii represent KTC (K+ transport coefficient), RKC (root K+ content), and SNaC/SKC (shoot Na+ content/shoot K+ content), respectively. Red dots represent significant SNPs associated with target traits.
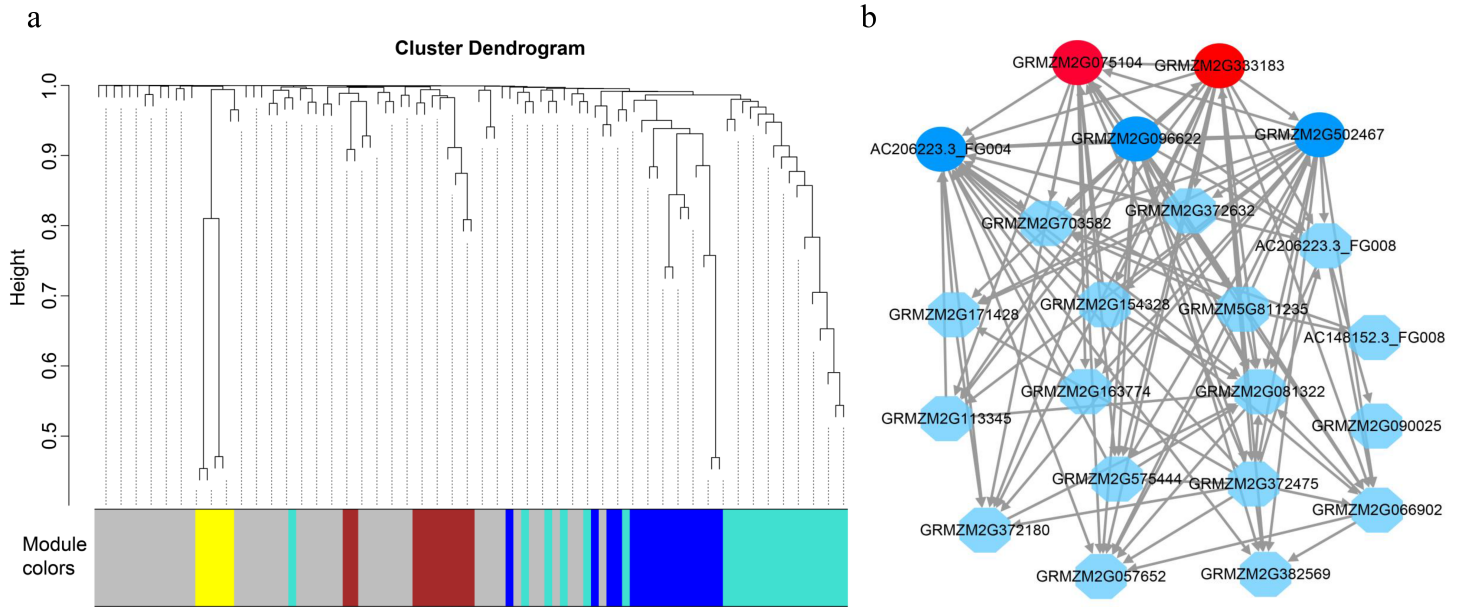
Figure 3

Modules and regulation networks identified in this study. (a) Modules identified by WGCNA. WGCNA represents weighted gene co-expression network analysis. Blue, brown, turquoise, and yellow colors represent the corresponding four modules. (b) Regulation networks of the two hub genes in turquoise module.
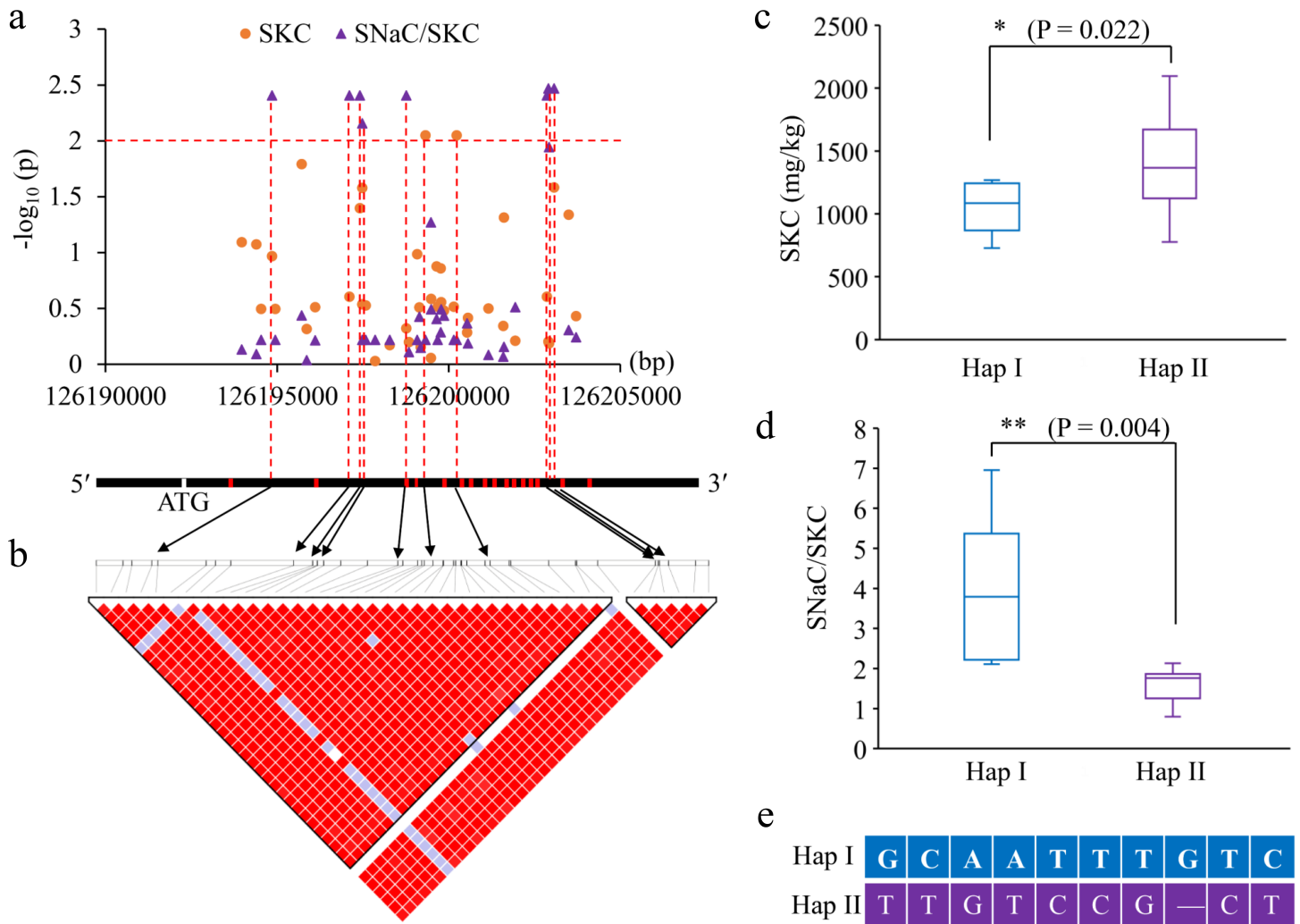
Figure 4

Candidate gene association analysis of GRMZM2G075104. (a) Significant markers associated with SKC (shoot K+ content) and SNaC/SKC (shoot Na+ content/shoot K+ content). (b) Pairwise LDs (linkage disequilibriums) between the markers. (c) Comparison of SKC (shoot K+ content) between HapI (haplotype I) and HapII (haplotype II). * significant at P < 0.05. (d) Comparison of SNaC/SKC (shoot Na+ content/shoot K+ content) between HapI (haplotype I) and HapII (haplotype II). ** significant at P < 0.01. (e) Details of HapI (haplotype I) and HapII (haplotype II). "−"represents insertion or deletion.
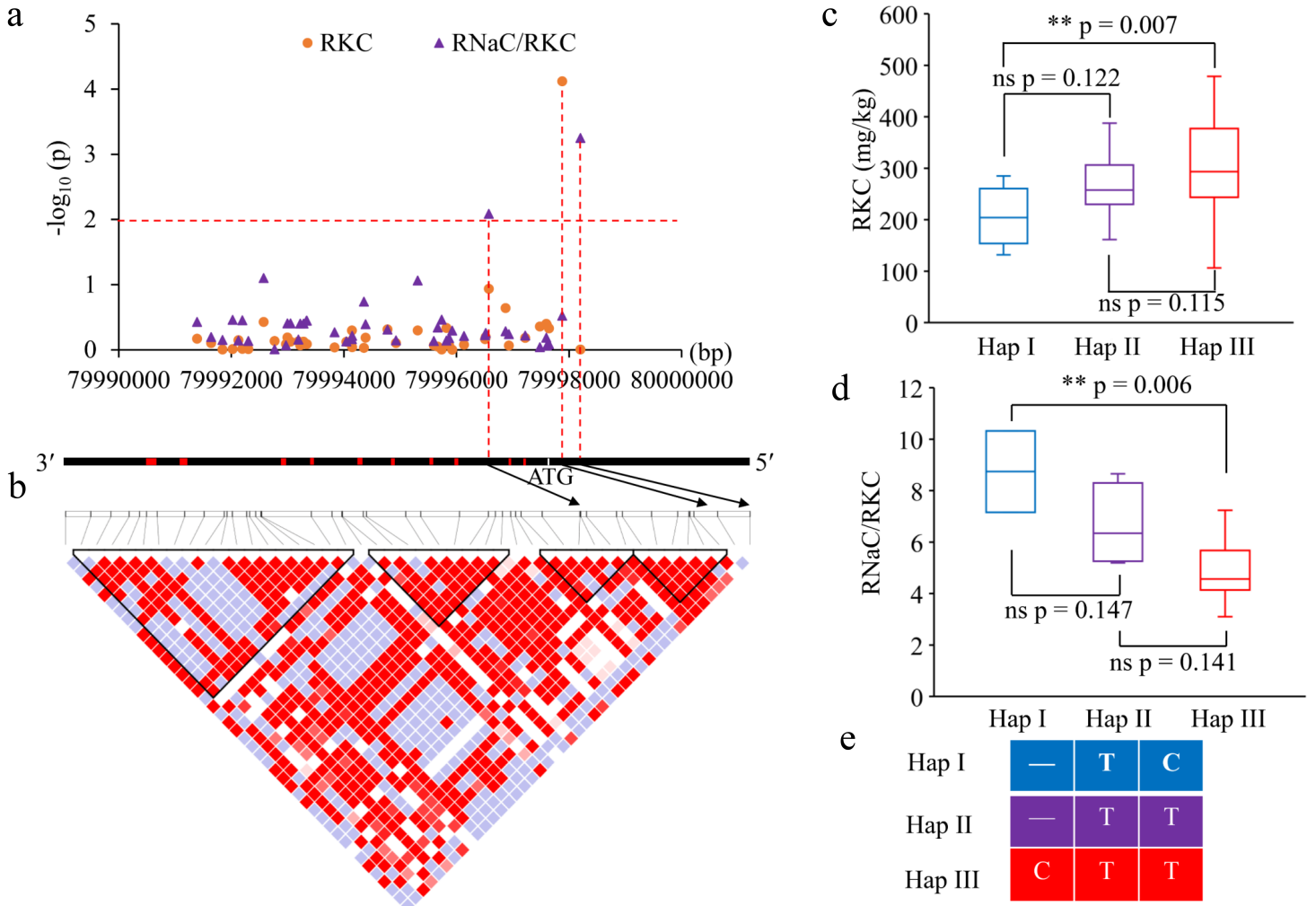
Figure 5

Candidate gene association analysis of GRMZM2G333183. (a) Significant markers associated with RKC (root K+ content) and RNaC/RKC (root Na+ content/root K+ content). (b) Pairwise LDs (linkage disequilibriums) between the markers. (c) Comparison of RKC (root K+ content) among HapI (haplotype I), HapII (haplotype II), and HapIII (haplotype III). ** significant at P < 0.01, ns = not significant. (d) Comparison of RNaC/RKC (root Na+ content/root K+ content) among HapI (haplotype I), HapII (haplotype II), and HapIII (haplotype III). ** significant at P < 0.01, ns = not significant. (e) Details of HapI (haplotype I), HapII (haplotype II), and HapIII (haplotype III). "−"represents insertion or deletion.
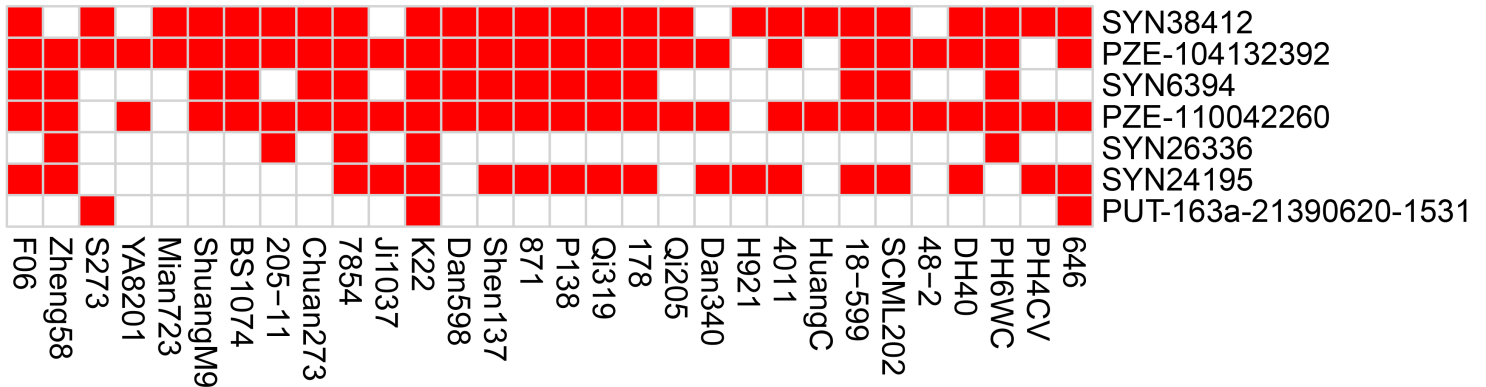
Figure 6

Distributions of superior SNP alleles among the 30 elite lines. Red and white represent superior and inferior alleles, respectively.

Supplementary Files

This is a list of supplementary files associated with this preprint. Click to download.

- supplementarymaterial.pdf